

Experimental and Numerical Study of Fatigue Crack Growth in Notched Specimens

G. Meneghetti¹, M. Zappalorto² and P. Lazzarin²

¹ Department of Mechanical Engineering, University of Padova, via Venezia 1 – 35131 Padova (Italy), giovanni.meneghetti@unipd.it

² Department of Management and Engineering, University of Padova, Stradella S. Nicola 3 – 36100 Vicenza (Italy), zappalorto@gest.unipd.it, plazzarin@gest.unipd.it

ABSTRACT. *The paper addresses the problem of crack propagation from notches, where different phenomena such as notch plasticity and the so-called short crack effect are superimposed and make the use of Linear Elastic Fracture Mechanics misleading. Tension-tension fatigue tests were conducted on notched specimens fabricated from 2-mm-thick FeP04 deep-drawing steel sheets. Different notch tip radii were considered, 0.2, 1.25, 2.5 and 10 mm. Crack propagation data show a discrepancy from the long crack behaviour described by the Paris law valid for the same load ratio. An interpretation of the short crack effect, at least at threshold conditions, based on the local strain energy density is put forward.*

INTRODUCTION

Early fatigue crack growth from notches is influenced by different phenomena, which makes the use of Linear Elastic Fracture Mechanics (LEFM) misleading (see for example [1] and references quoted therein), since experimentally observed crack growth rates do not conform to that expected by using the stress intensity factor concept. In fact in ductile metals cracks growing from notches might propagate within the notch plastic zone, at least during the early phase. Another source of deviation from the Paris' law is due to propagation of short cracks [2], which growth faster than expected from long cracks data making fatigue life prediction unsafe if based on standard long crack data.

In view of the above topics, the paper presents the experimental crack growth data measured in notched specimens cut from 2-mm-thick sheets made of FeP04 deep-drawing low carbon steel. Cracks emanated from notches having the tip radius ranging from 0.2 mm to 10 mm. The observed damage evolution at the notch tip is described. Crack growth data are presented in a standard crack propagation rate vs range of the mode I Stress Intensity Factor diagram, where the short crack behaviour, different from the long crack one, can be appreciated. A possible interpretation of the short crack behaviour is presented, which will be exploited in a future planned work.

EXPERIMENTAL TESTS

The considered material is a FeP04 deep-drawing steel widely used in automotive industry (ultimate tensile stress $\sigma_R=310$ MPa, yield stress $\sigma_{p02}=185$ MPa). Fatigue tests were carried out on 2-mm-thick single- and double-edge notched specimens (Figure 1). Notch tip radii ρ equal to 0.2, 1.25, 2.5 and 10 mm were considered.

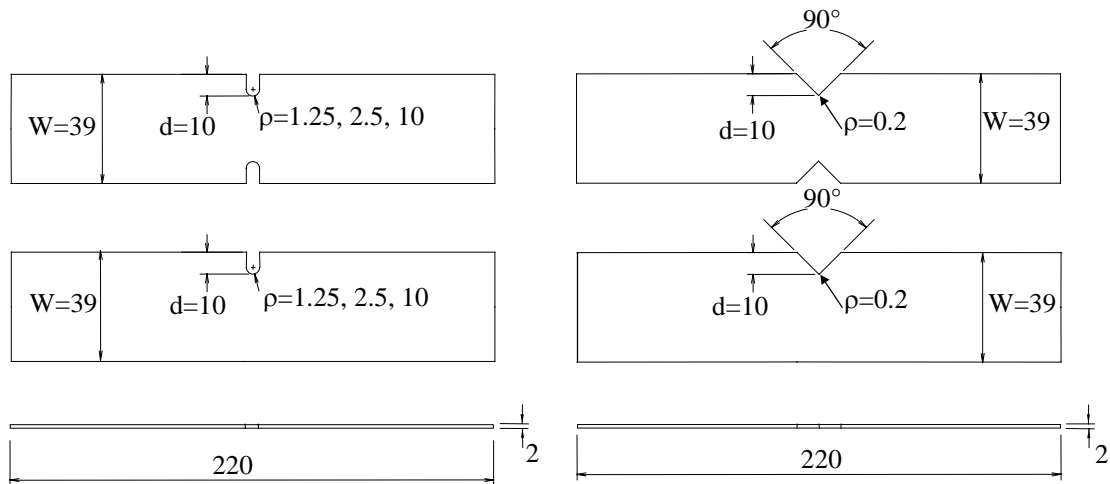


Figure 1. Geometries of the adopted single- and double edge-notched specimens. Size in mm.

Constant amplitude fatigue tests were conducted on a servo hydraulic testing machine MTS 810 equipped with a MTS Testar IIs controller. The nominal load ratio R (defined as the ratio between the minimum and the maximum applied load) was kept constant and equal to 0.1 for all tests. Crack propagation was monitored by means of a LEICA MZ6 stereoscope with a magnification factor 20x and a LEICA DFC280 digital camera, acquiring the images of the cracked specimen surfaces at prescribed intervals. The sampling rate was adjusted for each fatigue test as a function of the specimen geometry and the applied load level with the aim to describe in detail the entire crack propagation phase as close as possible. Images were finally processed to derive the crack length *versus* number of cycles data. Crack propagation rates were finally calculated according to the ASTM Recommendations [3].

FATIGUE TESTS RESULTS

Figures 2 summarise the experimental results obtained from single- and double-edge notched specimens. For a single test two symbols are used: open markers refer to the number of cycles necessary to initiate and propagate a crack up to 0.5 mm from the notch tip, while filled markers indicate the complete specimen failure. Being the scientific definition of crack initiation beyond the scope of the present work, the

diagram provides a rough separation of the ‘crack initiation’ phase from the subsequent ‘crack propagation’ phase. The critical length of 0.5 mm coincides with the El Haddad-Smith-Topper length parameter a_0 of the FePO4 steel material evaluated for $R=0.1$ [4].

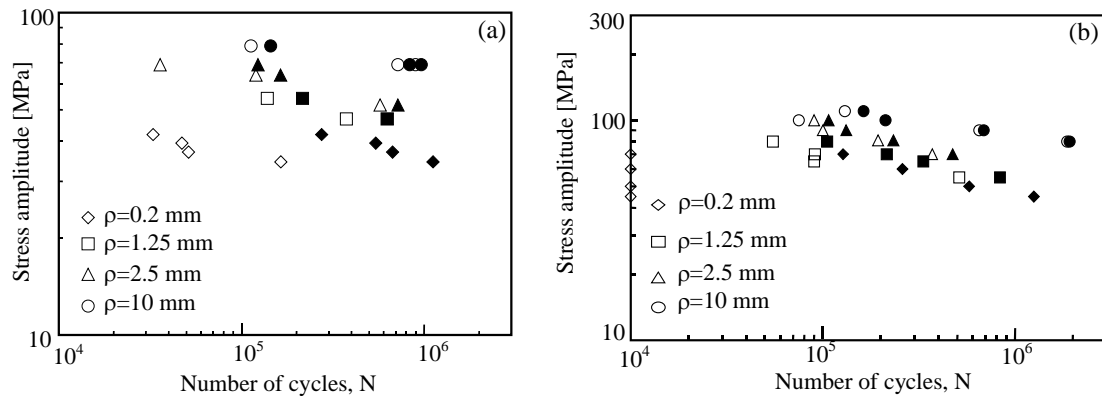


Figure 2. Summary of the experimental fatigue tests results in terms of net section stresses. Single edge notch (a) and double edge notch (b).

During the tests, fatigue damage was observed at the notch tip. In particular, in the specimens having 1.25, 2.5 and 10 mm notch tip radii, cracks initiated from different sites around the notch free edge in the proximity of the notch tip, highlighting that an entire volume of material was damaged by the fatigue process (Figure 3). Cracks initiated sometimes according to an inclined mode II path (stage I, according to Ref. [5]), similar to what observed in a carbon steel previously analysed by the authors [6]. Such an early stage of the fatigue damage process is documented by Figs. 4a), b) and c), showing different small fatigue cracks initiated at the notch tip zone. The figure reports also the fraction N/N_f of the fatigue life when the picture was taken, being N_f the total number of cycles to complete failure.

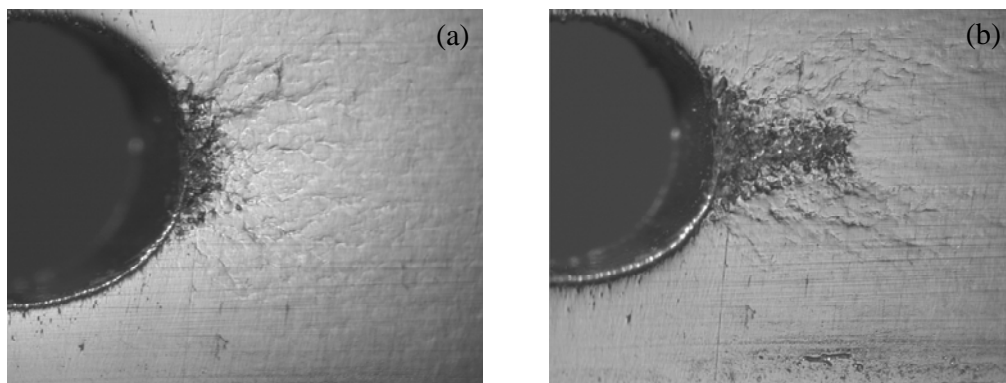


Figure 3. Fatigue damage in the proximity of the notch tip; $\rho=1.25$ mm, $\Delta\sigma_n = 160$ MPa $N_f= 210700$ cycles. $N/ N_f=0.35$ (a) and $N/ N_f=0.65$ (b).

After this early stage one single crack prevailed on the others and turned into a mode-I crack propagation path (stage II according to Ref. [5]), as depicted in Figs. 5 a), b) c), which report the same cracks shown by the previous Fig. 4 in a later stage of the fatigue tests. In sharply notched specimens having $\rho=0.2$ mm one single crack initiated from the notch tip and then propagated (Figures 4d and 5d).

For each crack length the range of the mode I Stress Intensity Factor (SIF) ΔK_I , defined as difference between the maximum value and the minimum value $\Delta K_I = (K_{I, \max} - K_{I, \min})$, was considered. Stress Intensity Factors were calculated by means of accurate two-dimensional Finite Element (FE) analyses under a plane stress hypothesis.

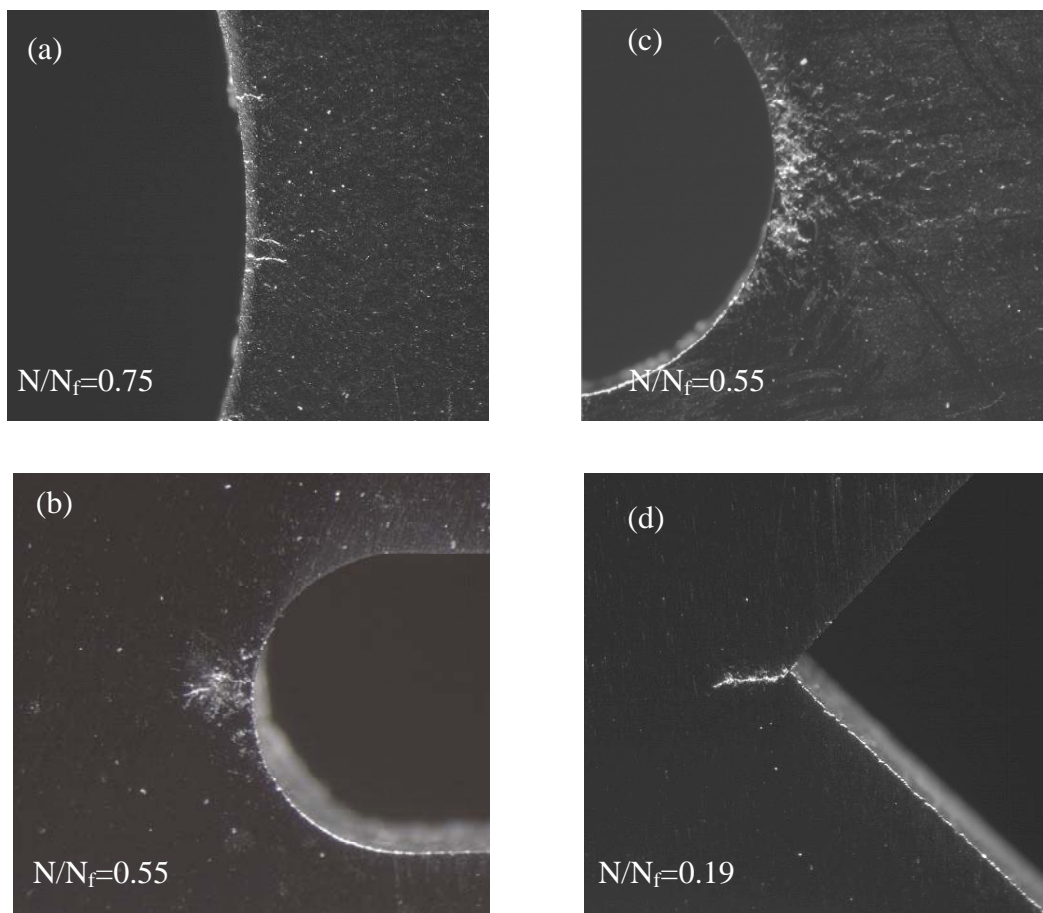


Figure 4. Early fatigue crack propagation observed in the sharp and blunt notches: $\rho=10$ mm, $\Delta\sigma_n = 200$ MPa $N_f= 211600$ cycles (a); $\rho=2.5$ mm, $\Delta\sigma_n = 140$ MPa $N_f= 120000$ cycles (b); $\rho=1.25$ mm, $\Delta\sigma_n = 160$ MPa $N_f= 105300$ cycles (c); $\rho=0.2$ mm, $\Delta\sigma_n = 120$ MPa $N_f=259400$ cycles d).

By considering a proper crack size increment in the numerical analyses, the obtained results could be interpolated to derive some closed-form expressions for the different

cracked geometries. In particular, for the double edge notched specimens with cracks propagating symmetrically from the two notches the expression is [4]:

$$\Delta K_I = \beta \cdot \Delta \sigma_g \cdot \sqrt{\pi \cdot (d + a)} \quad (1)$$

where $\Delta \sigma_g$ is the range of the nominal stress calculated over the gross area, d is the notch depth, a is the length of the notch-emanated crack (see Fig. 1) and β is a coefficient depending on the specimen geometry [4].

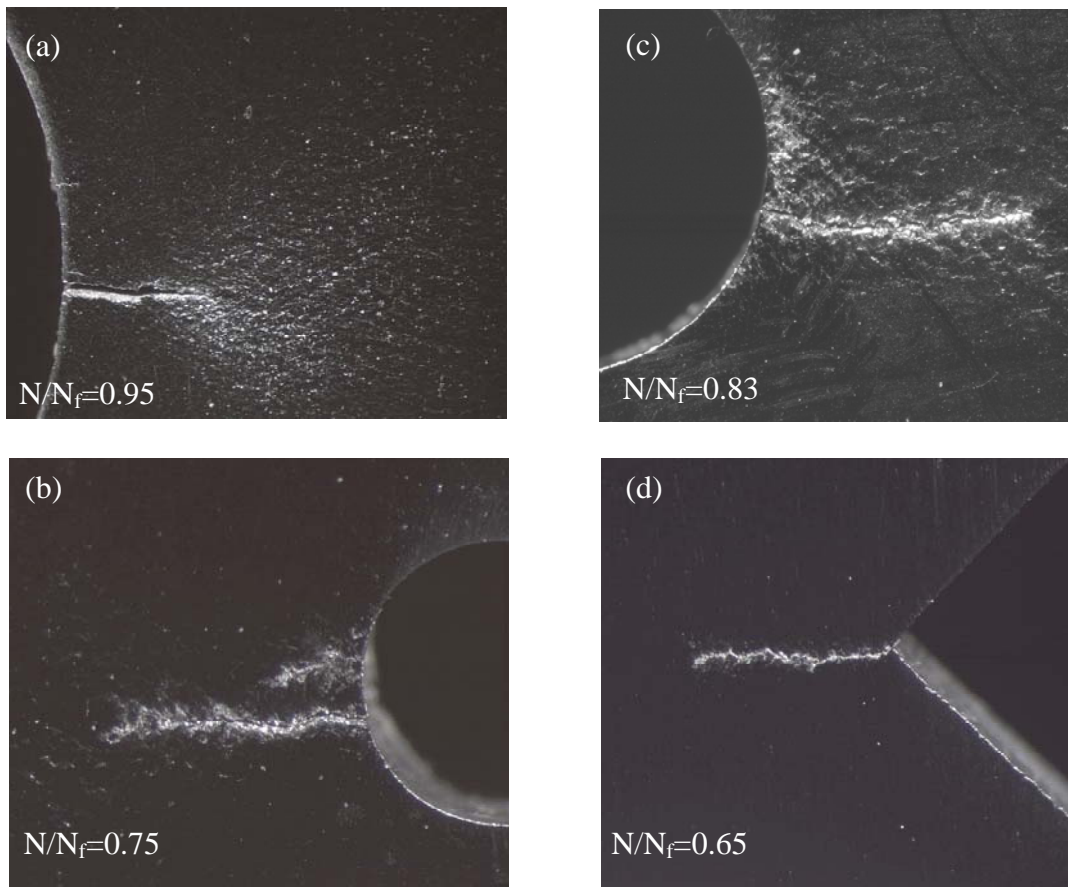


Figure 5. Fatigue crack propagation observed in the sharp and blunt notches later than reported in Fig. 3: $\rho=10$ mm, $\Delta \sigma_n = 200$ MPa $N_f= 211600$ cycles (a); $\rho=2.5$ mm, $\Delta \sigma_n = 140$ MPa $N_f= 120000$ cycles (b); $\rho=1.25$ mm, $\Delta \sigma_n = 160$ MPa $N_f= 105300$ cycles c); $\rho=0.2$ mm, $\Delta \sigma_n = 120$ MPa $N_f=259400$ cycles (d).

Sometimes the cracks did not propagate symmetrically from both notches, but propagation occurred on one side of the specimen only. In these cases, the following expressions were used [9]:

$$\Delta K_I = \Delta \sigma_g \sqrt{\pi(a+d)} \beta_1 \beta_2 \quad \beta_1 = \sqrt{1 - e^{-\beta}} \quad \beta = \frac{6a}{\rho} \left(1 + \frac{\rho}{W - 2d} \right) \quad (2)$$

$$\beta_2 = \frac{133}{310} \times 10^2 \times \psi^3 - \frac{137}{273} \times 10^2 \times \psi^2 + \frac{118}{515} \times 10^2 \times \psi - \frac{2141}{766}$$

where $\psi = \frac{a+2d}{W}$ and $1 \text{ mm} \leq a \leq 10 \text{ mm}$.

Finally, the SIFs for the single edge notched specimens have been evaluated according to the following expressions [9]:

$$\Delta K_I = \Delta \sigma_g \sqrt{\pi(a+d)} \alpha_1 \alpha_2 \quad (3)$$

where

$$\alpha_1 = \sqrt{1 - e^{-\beta}} \quad \beta = 7.75 \frac{a}{\rho} \left(1 + \frac{\rho}{W-d} \right) \quad (4)$$

$$\alpha_2 = -\frac{157}{447} \times 10^2 \times \psi^4 + \frac{53}{83} \times 10^2 \times \psi^3 - \frac{69}{169} \times 10^2 \times \psi^2 + \frac{65}{553} \times 10^2 \times \psi - \frac{5}{98}$$

In this last expression, $\psi = \frac{a+d}{W}$ and $0.35 \text{ mm} \leq a \leq 20 \text{ mm}$.

Figure 6 shows all the available crack propagation rates as a function of the range of the mode I SIF ΔK_I , as well as the fitted long crack Paris' law (of which the constant m and C are also reported). As a comparison, the long crack Paris' law previously derived by the authors for the same material is plotted too [4]. The figure highlights the well-known and anomalous crack growth behaviour of short cracks, of which the propagation rate is higher than that predicted by the long crack law for the same applied SIF range. Differently, when cracks grow up to a certain distance far from the notch tip, their propagation behaviour collapse onto the long crack behaviour. It should be noted that data for single edge notched specimens refer to crack length lower than 10 mm. Above such a length, the loading condition applied by the testing system differs too much from that simulated in the numerical model, which in turn is realistic for crack lengths shorter than about 10 mm.

DISCUSSION

Short crack behaviour is widely addressed in the technical literature, since the pioneering work due to El Haddad-Smith-Topper [2]. Explanations of their higher than expected propagation rates or, at threshold conditions, lower threshold values than expected from LEFM are usually based on crack closure development considerations,

leading to synthesis of experimental data based on the effective SIF range ΔK_{eff} .

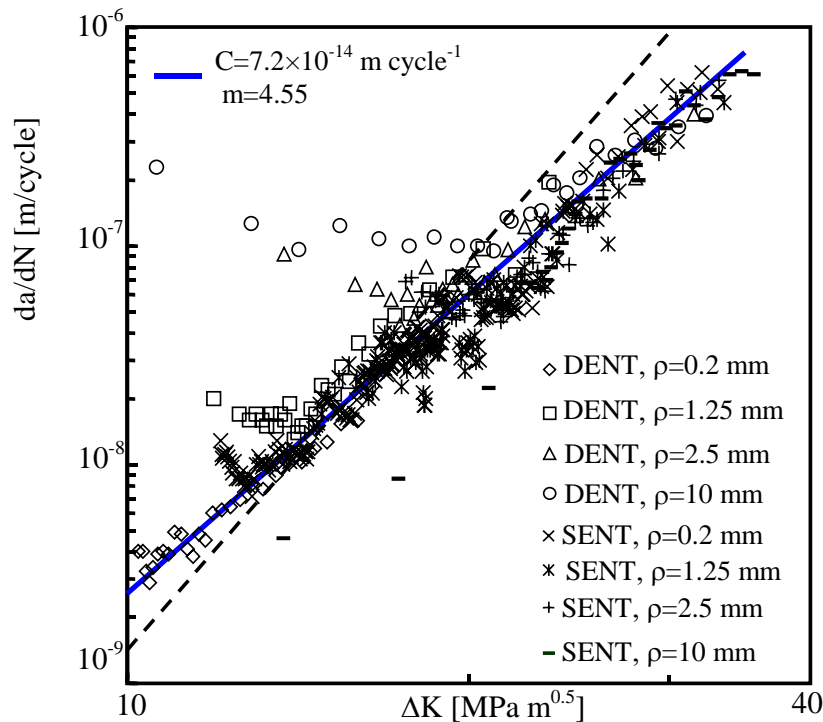


Figure 6. Crack growth data collected from the experimental tests on double-edge-notched specimens (DENT) and single-edge-notched specimens (SENT) and fitted long crack Paris' law (solid line); comparison with the long crack Paris' law previously derived in [4] for the same material (dashed line).

Recently Lazzarin and Berto interpreted the short crack effect on the fatigue limit of materials by considering the mean value of the strain energy density $\Delta\bar{W}$ evaluated over a well-defined 'structural volume' of radius R_c surrounding the crack tip [7]. By evaluating $\Delta\bar{W}$ from FE analyses, which accounts for the entire stress distribution, and not on the basis of the K_I parameter only, they showed that the threshold condition for a material containing a crack of diminishing size can be predicted exactly in the form of the Kitagawa diagram [8], as reported in Fig. 7. On these basis the threshold conditions for a notch-emanated crack and the short crack propagation problem will be dealt with in a future work [9].

CONCLUSIONS

The paper has presented the experimental results of Fracture Mechanics experiments conducted on notched specimens with different notch tip radii with the same notch depth. In blunt notches (notch radii equal to 1.25, 2.5 and 10 mm) multiple crack

initiation sites along the free edge in the proximity of the notch tip were observed. After that phase, one single dominant crack propagated until the specimen failure. In sharply notched specimens (notch radius equal to 0.2 mm) one single crack initiated at the notch tip and then propagated. The so-called short crack effect, i.e. higher propagation rates than predicted by the Linear Elastic Fracture Mechanics, was observed for all specimens. An interpretation of this phenomenon based on the mean value of the strain energy density in a structural volume surrounding the crack tip will be exploited in a future work.

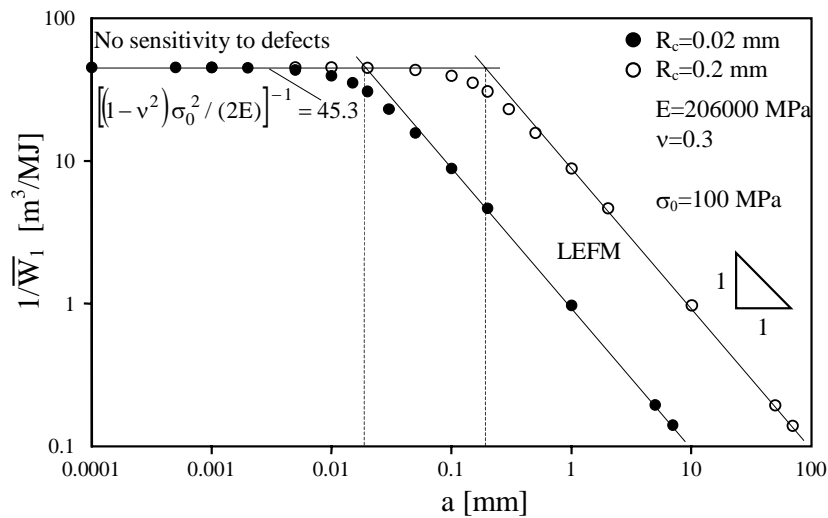


Figure 7. Threshold condition for a crack in terms of mean value of the strain energy density in a small ‘structural volume’ surrounding the crack tip [7].

REFERENCES

1. Jones, K.W., Dunn, M.L. (2009) *Int. J. Fatigue* **31**, 223-230.
2. El Haddad, M.H., Smith, K.N. and Topper, T.H. (1979) *J. Engng Mat. and Tech.* **101**, 42-46.
3. ASTM E 647-00, American Society for Testing and Materials.
4. Lazzarin, P., Tovo, R. and Meneghetti, G (1997) *Int. J. Fatigue* **19**, 647-657.
5. Miller K.J. (1993) *Fatigue Fract. Engng Mater. Struct.* **16**, 931-939.
6. Meneghetti, G., Susmel, L. and Tovo, R. (2007) *Eng. Fail. Anal.* **14**, 656-672.
7. Lazzarin, P., Berto, F. (2005) *Int. J. Fracture* **135**, L33-L38.
8. Kitagawa, H., Takahashi, S. (1976). In: *Proc. 2nd Int. Conference on Mechanical Behaviour of Materials*, pp. 627-631.
9. Meneghetti, G., Zappalorto, M. and Lazzarin, P. (2009) manuscript in preparation.